Obs.: In Eqs. (7), (8), and (13--18) one should read cot(tethaF/2) instead of cot(thetaF), thetaF with the appropriate subscripts.

Shaping Axis-Symmetric Dual-Reflector Antennas by Consecutively Concatenating Conic Sections

Fernando J. S. Moreira
Dept. Electronics Engineering - UFMG
Belo Horizonte, MG 31270-901
Email: fernandomoreira@ufmg.br

José R. Bergmann
CETUC - PUC-Rio
Rio de Janeiro, RJ 22453-130
Email: bergmann@cetuc.puc-rio.br

***Abstract*—This work presents the shaping of axis-symmetric dual-reflector antennas with a uniform-phase aperture illumination. The shaping procedure is based on the consecutive concatenation of conic sections, in order to provide a desired aperture-field distribution under geometrical optics (GO) principles. The procedure is simple, has fast numerical convergence, and is valid for any circularly symmetric dual-reflector configuration. To illustrate the shaping procedure, an axis-displaced Cassegrain (ADC) is designed to provide a uniform aperture illumination. The GO shaping results are validated using accurate method-of-moments analysis.**

I. Introduction

Recently, a procedure for the reflector shaping of circularly symmetric dual-reflector antennas has been presented [1]. The procedure is based on the consecutive concatenation of conic sections to describe the generatrices of the sub- and main-reflectors, in order to provide an aperture illumination with a uniform phase distribution together with a prescribed amplitude distribution. The procedure improves traditional methods [2],[3] as no ordinary differential equation must be solved to obtain the shaped reflector surfaces. The technique also provides an one-step procedure, improving the two-step procedure based on ray tracing developed in [4].

However, in [1] the authors adopted rectangular coordinates to describe the conic sections employed in the representation of the shaped-reflector generatrices. For that reason, the one-step procedure presented in [1] is based on a nonlinear algebraic equation, which was approximated to provide simple iterative solution.

In the present work we improve the formulation in [1] by using polar coordinates to represent the conic sections. The present procedure renders a one-step iterative procedure with simple linear algebraic equations, thus avoiding any approximation to attain the numerical solution besides the conic representation of the reflector generatrices. Another interesting feature of the present formulation is that it is valid for any axis-symmetric dual-reflector configuration.

In the next section the formulation based on conic sections is presented. Then, a configuration based on an axis-displaced Cassegrain (ADC) is adopted to illustrate the usefulness of the procedure. The ADC-like antenna is shaped to provide the uniform illumination of the aperture. We investigate the convergence of the procedure compared to another where an ordinary differential equation is numerically integrated to obtain the shaped surfaces [3]. The radiation characteristics of the antennas are numerically obtained by a method-of-moments (MoM) analysis in order to validate the applicability of the proposed shaping technique, which is based on geometrical optics (GO) concepts.

This work was supported by CNPq, CAPES, FAPEMIG, and FAPERJ, Brazil.

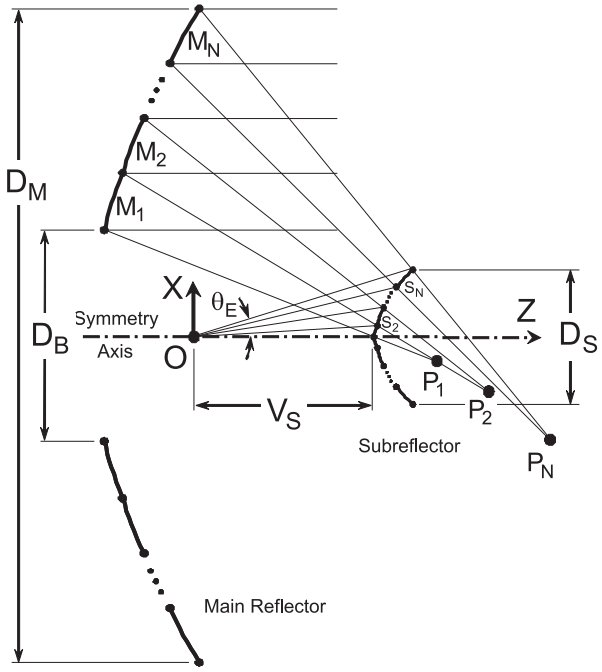

Fig. 1. Dual-reflector shaping by consecutive conic sections.

II. Shaping-Procedure Formulation

The basic idea is to represent the reflector generatrices by conic sections consecutively concatenated, as depicted in Fig. 1. Notice that an ADC-like configuration will be adopted to illustrate and derive the shaping formulation, but the final procedure is valid for any one of the four axis-symmetric dual-reflector configurations [5],[6].

The conic sections describing the subreflector ($S_n, n = 1, \ldots, N$) have two focci. One is always at the origin O (where

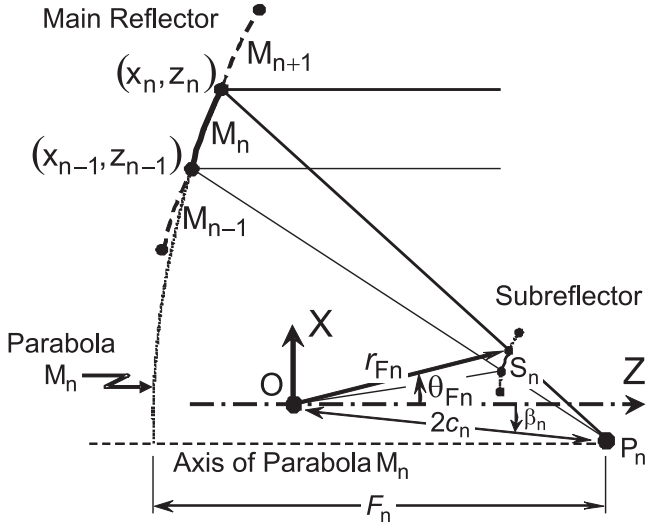

Fig. 2. Conic-section parameters.

the feed phase-center is assumed to be) and another at P_n. As n is varied from 1 to N, P_n spans the locus of the subreflector caustic. P_n is also the focus of the parabola section M_n that describes a portion of the main reflector. The parabola axis, passing through P_n, is always parallel to the symmetry axis of both reflectors (z axis), such that all main-reflector rays arrive parallel to each other at the antenna aperture plane, providing a uniform phase distribution according to GO principles. Another GO principle that will be used to define the conic sections is that the energy contained in the bundle of rays departing from O and intercepting the subreflector conic section S_n is conserved at the antenna aperture after being reflected by the corresponding main-reflector parabola M_n.

In order to uniquely define sections S_n and M_n, four parameters must be determined: the focal distance F_n of the parabola section M_n, the interfocal distance (i.e., the distance between O and P_n) $2c_n$ and the eccentricity e_n of the subreflector conic S_n, and the tilt angle β_n of the axis of S_n with respect to the z-axis (see Fig. 2). So, four equations are needed.

From the polar equation of S_n one obtains the following relation:

$$r_{Fn} = \frac{c_n(e_n - 1/e_n)}{e_n \cos(\beta_n - \theta_{Fn}) - 1} = \frac{a_n}{b_n \cos\theta_{Fn} + d_n \sin\theta_{Fn} - 1} , \quad (1)$$

where

$$a_n = c_n(e_n - 1/e_n) , \quad (2)$$

$$b_n = e_n \cos\beta_n , \quad (3)$$

$$d_n = e_n \sin\beta_n , \quad (4)$$

θ_{Fn} is the feed ray direction (with respect to the z-axis) toward the superior extreme of S_n (see Fig. 2), and r_{Fn} is the distance from O to S_n along the ray-direction θ_{Fn}. The first equation of the shaping procedure is obtained from (1):

$$r_{Fn-1} = \frac{a_n}{b_n \cos\theta_{Fn-1} + d_n \sin\theta_{Fn-1} - 1} , \quad (5)$$

where θ_{Fn-1} and r_{Fn-1} are known from the previous step $(n-1)$. The iterative process starts at $n = 0$ with $\theta_{F0} = 0$ and $r_{F0} = V_S$, where V_S is the desired distance between the feed phase-center and the subreflector apex (see Fig. 1). Observe that the variable θ_{Fn} controls the steps of the shaping iterative procedure and is uniformly varied from $\theta_{F0} = 0$ to the subreflector edge at $\theta_{FN} = \theta_E$, such that $\Delta\theta_F = \theta_{Fn} - \theta_{Fn-1} = \theta_E/N$. In principle, the accuracy of the shaping procedure is increased by decreasing $\Delta\theta_F$.

The second shaping equation is obtained by enforcing a constant path length ℓ_o from O (i.e., from the feed phase center) to the aperture plane (assumed at $z = 0$) to ensure a uniform phase distribution. From the polar equations of S_n and M_n one can show that

$$\ell_o = 2F_n + \frac{2c_n}{e_n} - 2c_n \cos\beta_n = 2F_n + \frac{2c_n}{e_n}(1 - b_n) . \quad (6)$$

The constant path length ℓ_o must be specified *a priori*. For design purposes, notice that ℓ_o is approximately equal to twice the distance between sub- and main-reflectors.

The remaining equations are obtained from the conservation of energy and from the mapping relation between the feed ray direction θ_F and the aperture Cartesian coordinate x (which is also the x coordinate of the main reflector). The mapping relation between θ_F and x is given by [7]:

$$\frac{x_n}{\ell_o} = \frac{1 + b_n + 2a_n/\ell_o - d_n \cot\theta_{Fn}}{d_n + (b_n - 1)\cot\theta_{Fn}} . \quad (7)$$

So, from (7) at $\theta_F = \theta_{Fn-1}$ one obtains the third shaping equation:

$$\frac{x_{n-1}}{\ell_o} = \frac{1 + b_n + 2a_n/\ell_o - d_n \cot\theta_{Fn-1}}{d_n + (b_n - 1)\cot\theta_{Fn-1}} , \quad (8)$$

where x_{n-1} is the main-reflector x coordinate obtained in the previous iteration (see Fig. 2).

In order to use (7) as the forth shaping equation, one must obtain the new coordinate x_n of the main reflector. This is accomplished by applying the conservation of energy along the tube of rays that departs from O (the location of the feed phase-center) and arrives at the aperture plane after being reflected by both sub- and main-reflectors. The conservation of energy is mathematically described by the following integral:

$$\int_0^{\theta_{Fn}} G_F(\theta_F)\, r_F^2 \sin\theta_F \, d\theta_F = N_F \int_{D_B/2}^{x_n} G_A(x)\, x \, dx \quad (9)$$

where $G_F(\theta_F)$ is the circularly-symmetric radiated feed power density, $G_A(x)$ is the desired aperture power density, and

$$N_F = \frac{\int_0^{\theta_E} G_F(\theta_F)\, r_F^2 \sin\theta_F \, d\theta_F}{\int_{D_B/2}^{D_M/2} G_A(x)\, x \, dx} \quad (10)$$

is a normalization factor that assures that all feed power intercepted by the subreflector is conserved at the antenna

aperture. In (9) and (10), D_B is the projected diameter of the main-reflector opening and D_M is the projected main-reflector diameter (see Fig. 1). Both D_M and D_B are input parameters for the shaping process. In principle, $D_B > D_S$ to avoid the subreflector blockage of the main-reflector reflected rays and also to allow the feed access to the principal focus (O) of the dual-reflector system (see Fig. 1). Observe that, for $n = 0$, $x_n = D_B/2$. After x_n is numerically calculated from (10), the forth shaping equation is (7).

Substituting (5) and (6) into (7) and (8) one obtains the following linear system:

$$f_1 b_n + g_1 d_n = h_1 \tag{11}$$
$$f_2 b_n + g_2 d_n = h_2 \tag{12}$$

where

$$f_1 = x_{n-1}\cot\theta_{Fn-1} - \ell_o - 2r_{Fn-1}\cos\theta_{Fn-1} \tag{13}$$
$$f_2 = x_n\cot\theta_{Fn} - \ell_o - 2r_{Fn-1}\cos\theta_{Fn-1} \tag{14}$$
$$g_1 = x_{n-1} + \ell_o\cot\theta_{Fn-1} - 2r_{Fn-1}\sin\theta_{Fn-1} \tag{15}$$
$$g_2 = x_n + \ell_o\cot\theta_{Fn} - 2r_{Fn-1}\sin\theta_{Fn-1} \tag{16}$$
$$h_1 = x_{n-1}\cot\theta_{Fn-1} + \ell_o - 2r_{Fn-1} \tag{17}$$
$$h_2 = x_n\cot\theta_{Fn} + \ell_o - 2r_{Fn-1}\ . \tag{18}$$

The solution of (11) and (12) gives

$$b_n = \frac{h_1 g_2 - h_2 g_1}{f_1 g_2 - f_2 g_1} \tag{19}$$
$$d_n = \frac{f_1 h_2 - f_2 h_1}{f_1 g_2 - f_2 g_1}\ . \tag{20}$$

The conic parameters are then calculated as follows. The parameters e_n and β_n are calculated from (3), (4), (19), and (20). Then, a_n and, consequently, $2c_n$ are calculated from (2) and (5). Finally, F_n is calculated from (6).

With the conic parameters determined, the subreflector point at $\theta_F = \theta_{Fn}$ is located by the vector

$$r_{Fn}\cos\theta_{Fn}\,\hat{z} + r_{Fn}\sin\theta_{Fn}\,\hat{x}\ , \tag{21}$$

where r_{Fn} is given by (1). The corresponding main-reflector point is located by the vector

$$z_n\,\hat{z} + x_n\,\hat{x}\ , \tag{22}$$

where the Cartesian coordinate z_n is given by the parabola equation of M_n:

$$z_n = \frac{(x_n - 2c_n\sin\beta_n)^2}{4F_n} - F_n + 2c_n\cos\beta_n\ . \tag{23}$$

Finally, the location of P_n at the subreflector caustic is given by the vector

$$2c_n\cos\beta_n\,\hat{z} + 2c_n\sin\beta_n\,\hat{x}\ . \tag{24}$$

The steps are repeated until $\theta_{FN} = \theta_E$ (i.e., $n = N$).

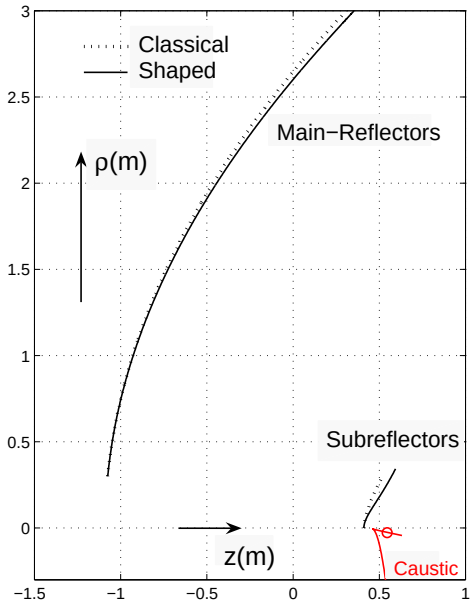

Fig. 3. Sub- and main-reflector generatrices of the classical (dotted lines) and shaped (solid lines) ADC's. The caustic refers to the shaped subreflector.

III. Other Dual-Reflector Configurations

The formulation derived in Sect. II assumed an ADC-like configuration, as illustrated in Figs. 1 and 2. For other dual-reflector configurations [5],[6] one should proceed as follows. For a dual-reflector configuration based on an axis-displaced Gregorian (ADG) one just needs to change the sign of x_n after calculation from (9). For an axis-displaced ellipse (ADE) configuration, the feed illumination toward the aperture is reversed. In this case, (9) must be replaced by

$$\int_0^{\theta_{Fn}} G_F(\theta_F)\, r_F^2\, \sin\theta_F\, d\theta_F = N_F \int_{x_n}^{D_M/2} G_A(x)\, x\, dx \tag{25}$$

where, for $n = 0$, $x_n = D_M/2$. Finally, for an axis-displaced hyperbola (ADH) configuration, one must use (25) to calculate x_n, changing its sign afterward.

IV. Results and Discussion

In oder to illustrate the procedure presented in Sect. II, an ADC-like configuration was shaped for a uniform aperture distribution. The configuration is exactly the second example presented in [1]. The shaped ADC antenna is compared against a classical ADC configuration with the following geometrical parameters: $D_M = 6$ m, $D_B = 0.6$ m, $D_S = 0.6$ m, $\ell_o = 3$ m, and $\theta_E = 30°$. From [6] one obtains $V_S = 0.409$ m. The operating frequency is 5 GHz, such that $D_M \approx 100\,\lambda$. The sub- and main-reflector generatrices of the classical ADC are illustrated with dotted lines in Fig. 3.

Applying the shaping procedure of Sect. II, the ADC configuration was shaped to provide a uniform amplitude distribution over the illuminated portion of the aperture (i.e., $G_A(x)$ constant from $x_0 = D_B/2$ to $x_N = D_M/2$). The feed

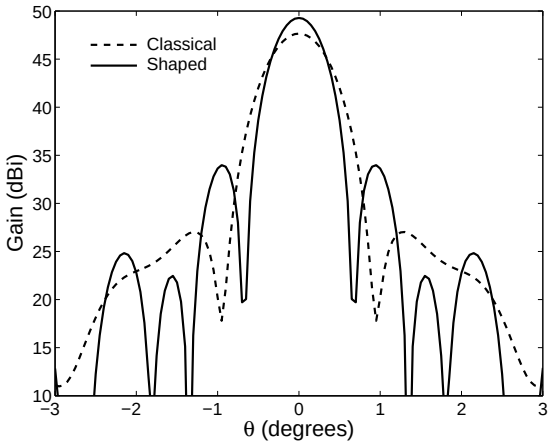

Fig. 4. E-plane radiation patterns of the classical (dashed lines) and shaped (solid lines) ADC's. Reflectors shaped with $\Delta\theta_F \approx 10^{-4} \times \theta_E$.

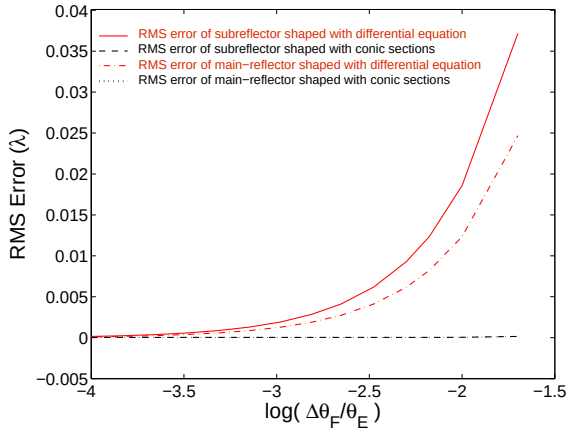

Fig. 5. RMS error of the shaped reflector surfaces as function of $\Delta\theta_F$.

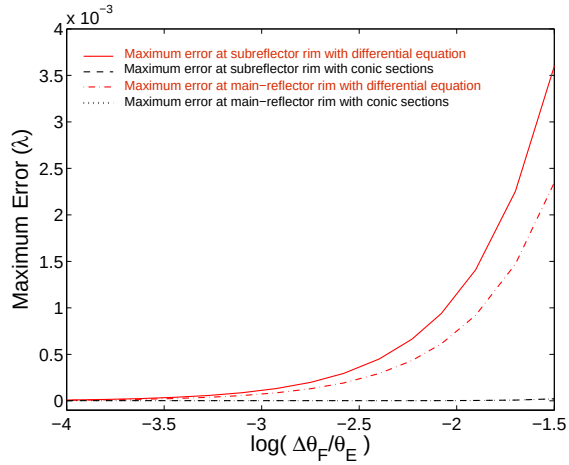

Fig. 6. Maximum error (at the reflector rims) of the shaped reflector surfaces as function of $\Delta\theta_F$.

is the same adopted in [1]:

$$G_F(\theta_F) = \cos^{2p}(\theta_F/2)/r_F^2 \ , \qquad (26)$$

with $p = 83$ to provide -25 dB taper at $\theta_F = \theta_E$ [1]. The shaped reflector generatrices are plotted with solid lines in Fig. 3 together with the shaped subreflector caustic.

Both classical and shaped antennas, fed by the feed model of (26), were analyzed by a MoM technique. The radiation patterns in the E-plane are depicted in Fig. 4. As expected, the gain of the shaped antenna (49.28 dBi) is higher that that of the classical configuration (47.65 dBi). The side-lobe levels of the shaped antenna are also higher (about 7 dB) than those of the classical configuration, as expected.

The shaping procedure of Sect. II is simpler and, consequently, faster than traditional procedures based on the numerical integration of ordinary differential equations [2],[3]. Another important feature is the numerical convergence of the present procedure, which provides the same accuracy of traditional procedures with $\Delta\theta_F$ steps about 1000 times bigger. To illustrate this, Fig. 5 presents the RMS error of the shaped reflector surfaces as function of $\Delta\theta_F$. The *reference* surfaces are obtained from a traditional shaping procedure [3] with a very small $\Delta\theta_F$ value ($\Delta\theta_F \approx 10^{-4} \times \theta_E$). The RMS errors of the shaped subreflectors were obtained by comparing the values of r_F (i.e., the distance from O to the subreflector) with those of the reference subreflector. For the main reflectors, the comparisons were made with the Cartesian z coordinates. From Fig. 5 one observes that the shaping procedure of Sect. II sustains very small RMS errors even for $\Delta\theta_F \approx \theta_E/50$ (i.e., with approximately $N = 50$ conic sections representing each reflector surface).

As both shaping procedures (based on differential equations or conic sections) are iterative processes, the surface error tends to increase as $\theta_F \to \theta_E$ (i.e., at the reflector rims). Figure 6 shows the maximum error (at the reflector rims) as function of $\Delta\theta_F$. By comparing Figs. 5 and 6 one observes that both errors have approximately the same convergence behavior (i.e., the RMS error is actually dominated by the maximum error at the reflector rims).

REFERENCES

[1] Y. Kim and T.-H. Lee, "Shaped Circularly Symmetric Dual Reflector Antennas by Combining Local Conventional Dual Reflector Systems," *IEEE Trans. Antennas Propagat.*, vol. 57, no. 1, pp. 47–56, Jan. 2009.

[2] V. Galindo, "Design of dual-reflector antennas with arbitrary phase and amplitude distributions," *IEEE Trans. Antennas Propagat.*, vol. AP-12, no. 4, pp. 403–408, July 1964.

[3] J. J. Lee, L. I. Parad, and R. S. Chu, "A shaped offset-fed dual-reflector antenna," *IEEE Trans. Antennas Propagat.*, vol. AP-27, no. 2, pp. 165–171, Mar. 1979.

[4] J. Hakli, J. Ala-Laurinaho, and A. V. Raisanen, "Numerical synthesis method for designing a shaped dual reflector feed system," *Proc. Inst. Elect. Eng. Microw. Antennas Propag.*, vol. 152, no. 5, pp. 311-318, Oct. 2005.

[5] S. P. Morgan, "Some examples of generalized Cassegrainian and Gregorian antennas," *IEEE Trans. Antennas Propagat.*, vol. AP-12, no. 6, pp. 685-691, Nov. 1964.

[6] F. J. S. Moreira and Aluizio Prata, Jr., "Generalized classical axially symmetric dual-reflector antennas," *IEEE Trans. Antennas Propagat.*, vol. 49, no. 4, pp. 547–554, April 2001.

[7] B. S. Westcott, F. A. Stevens, and F. Brickell, "GO synthesis of offset dual reflectors," *IEE Proc.*, Pt. H, vol. 128, no. 1, pp. 11–18, Feb. 1981.